PCCP

Accepted Manuscript

ROYAL SOCIETY OF CHEMISTRY

www.rsc.org/pccp

Key Factors in Determining the Arrangement of π-Conjugated Oligomers inside Carbon Nanotubes

Takashi Yumura* **and Hiroki Yamashita**

Department of Chemistry and Materials Technology, Kyoto Institute of Technology, Matsugasaki, Sakyo-ku, Kyoto, 606-8585, Japan

*To whom all correspondence should be addressed. E-mail; yumura@kit.ac.jp

(Takashi Yumura)

†Kyoto Institute of Technology (KIT)

Abstract: Density functional theory (DFT) calculations with dispersion corrections elucidated key factors for determining the arrangement of π–conjugated oligomers inside a carbon nanotube. The current study considered methyl-terminated terfurans as guests inside a host tube; the results were compared with those obtained in previous studies for methyl-terminated terthiophenes inside a nanotube. DFT calculations found that the most important factor in determining the guest arrangement is the host-guest interactions arising from long-range CH–π and π–π interactions. Particularly, the host-guest interactions play a crucial role in the arrangement of π-conjugated oligomers inside a larger-diameter tube: π-conjugated oligomers sit near the inner tube wall to maximize attractive host-guest interactions. Within a smaller-diameter tube, host-guest interactions as well as guest-guest (interchain) interactions are responsible for the guest arrangement. Then, stronger host-guest (weaker guest-guest) interactions are a major (minor) factor. The stronger host-guest interactions are sufficient to deform the inner π-conjugated oligomers. Due to the tube encapsulation, inner terfurans lose their planarity, leading to a weakening of the interchain interactions. In contrast, tube encapsulation induces terthiophenes to assume nearly planar structures, enhancing their interchain interactions. As a result, the magnitude of the interchain interactions is dependent on types of inner oligomer. Reflecting the different interchain interactions, multimeric terfurans inside a nanotube exhibit molecular packings that are different from those of corresponding terthiophenes. Considering the importance of the arrangement of inner π-conjugated oligomers for their electronic properties, and thus nanotube containers can tune the properties of inner oligomers.

1. Introduction

Various π-conjugated oligomers have attracted much attention because of their use in solar cells.[1–7] Their properties are influenced by the gap between the highest occupied molecular orbital (HOMO) and the lowest unoccupied molecular orbital (LUMO) of an individual oligomer, as well as by molecular packing in the solid state. Molecular packing is important because it determines the strength of intermolecular interactions between adjacent oligomers that are responsible for their charge transfer properties. For example, the most famous oligothiophenes (Chart 1) usually assume herringbone structures, although cofacial structures were sometimes observed in the crystal structures of oligothiophene oligomers substituted by bulky groups as well as in the crystal structures of oligomers with both electron-rich and electron-deficient aryl rings.[1–7] Recently, oligofurans (Chart 1), with frameworks that are more rigid than those of oligothiophene for twisting adjacent five-membered rings, have been successfully synthesized.[8–10] In their crystal form, planar oligofurans are packed in herringbone motifs.

Control of molecular packing is important for regulation of charge transfer rates between π conjugated oligomers.[11–16] The use of the inner space of a carbon nanotube is one of the most promising strategies for this purpose.[17–30] There have been some reports on thiophene oligomers contained inside the nanotubes.[24–29] The use of their restricted space is advantageous because the movement of the thiophene guest molecule is highly restricted: the oligomer guests are allowed to easily move only along the tube-axis direction. Furthermore, the guest structures are influenced by the interactions with

the host tube, and therefore the host-guest interactions determine the guest arrangements. Due to the advantages of the nanometer-sized environment, the number of guest arrangements would be limited, and therefore it may be possible to control the electronic properties of guest molecules by utilizing nanotube confinement.[31,32]

Following this approach, we performed quantum chemical calculations based on density functional theory (DFT) to investigate how multimeric methyl-terminated terthiophenes (3T) orient inside a nanotube through host-guest interactions.[31,32] DFT calculations including dispersion corrections (B97-D functional) found a variety of arrangements of the thiophene guests inside the tube host; these arrangements depend on host-tube diameter as well as on the number of guests, as shown in Figure 1. Reflecting the various thiophene arrangements on the inside of a nanotube, inner thiophene oligomers exhibit a variety of different interactions. The interchain interactions split the orbitals that are constructed from the frontier orbitals of the single chain, and therefore nanotube confinement has a strong impact on the arrangements and electronic properties of the inner terthiophene chains.

The present study extends our previous DFT studies to investigate multimeric oligofuran chains inside a nanotube. As mentioned above, oligofurans have planar structures that allow π electrons to delocalize over the framework; such structures are different from thiophene oligomers where five-membered rings are slightly twisted. However, the ready degradation of oligofurans upon exposure to a combination of light and dioxygen is a significant drawback.[8] This unfavorable feature prevents the use of oligofurans as organic electronic materials. To overcome this drawback, we propose

that carbon nanotubes can act as nanocontainers, allowing inner oligofurans to exist in their ground state by preventing dioxygen from attacking them. This hypothesis originated from an analogy with the previous studies.[31,32] Following this hypothesis, the current study aims to obtain the electronic properties of multimeric oligofuran inside nanotubes with a diameter ranging from 10.9 to 13.7 Å; we then compared our results with the results for thiophene molecules inside a nanotube.

2. Calculation Method

In the current study, we discuss structural and electronic properties of multimeric oligofurans inside an armchair carbon nanotube, as shown in Figure 2. We constructed the nanotube models by using (8,8) and (10,10) nanotubes terminated with H atoms ($C_{304}H_{32}$ and $C_{380}H_{40}$, 22.1 Å length). These nanotube clusters are large enough to accurately model the electronic properties of the corresponding infinitely long nanotubes.[33–39] Following the previous studies,[31,32] we considered methyl-terminated oligomers consisting of three furan rings (terfuran, 3F). Accordingly, we will use the notation of n×3F@(m, m) throughout this study as an abbreviation for an armchair (m, m) nanotube containing n terfurans.

As discussed in the previous reports,[31,32] interactions between a host tube and π conjugated guests arise from the long range π–π interactions and CH–π interactions. To correctly describe such long-range interactions in DFT calculations, a suitable functional must be carefully chosen. Therefore, the B97D functional that includes a dispersion correction in a GGA-based B97 functional[40,41] was selected for the current

study rather than the popular B3LYP functional.[42–46] On the other hand, GGA-based DFT calculations are well known to underestimate HOMO-LUMO gap, in contrast to B3LYP calculations that accurately reproduce the experimentally obtained gaps.[47–49] Considering the advantages and disadvantages of the B97D and B3LYP functionals, we chose the following procedure to investigate the geometrical and electronic properties of multimeric methyl-terminated terfurans inside nanotubes. We first optimized n×3F@(m,m) structures by using the B97D functional. We then used the B3LYP functional to perform single-point calculations of the B97D optimized n×3F@(m,m) structures to obtaining the orbital energy levels and orbital distributions, focusing especially on the orbitals derived from the multimeric terfurans within the nanotubes.[31,32] To select basis sets that are suitable for large-scale calculations of n×3T@(m,m), we used the 6-31++G** basis set[50-52] for the thiophene oligomers and the 6-31G** basis set[50,51] for the finite-length tube models. Accordingly, the optimization of the nanotubes containing some terfurans involved up to 7032 contracted basis functions. All calculations were performed using the Gaussian 09 program.[53]

3. Results and Discussion

Properties of terfuran and terthiophene

We first discuss the properties of methyl-terminated terfurans and compare them to those of methyl-terminated terthiophene. Figure 3 displays the optimized structures together with charges calculated by natural populations analysis (NPA).[54] As shown in Figure 3(a), bond-length alternation patterns of terfuran are almost the same as those of

terthiophene. Figure 3(b) presents the orbital distributions of the frontier orbitals of the two π-conjugated oligomer types. Similar frontier orbital distributions can be found for terfuran and terthiophene. The HOMO-LUMO energy gaps were calculated to be 3.55 and 3.24 eV for terfuran and terthiophene, respectively. Despite the similarity between the geometrical and orbital properties of the two oligomers, they contain heteroatoms with different signs of the charges; calculated NPA charges on oxygen atoms in 3F are ~ –0.47, whereas the charges on sulfur atoms in 3T are ~ 0.44. The different signs of their calculated NPA charges can be understood based on the electronegativity differences between the heteroatoms and carbon atoms.[55]

These differences are important for determining the twisting potential energies of the π-conjugated oligomers. Figure 4(a) displays potential energy surfaces of the π-conjugated oligomers as a function of dihedral X–C–C–X angles (θ) where X is O or S. Dihedral angle dependent HOMO-LUMO gaps are also shown. Figure 4(b) shows that the HOMO-LUMO gaps increase as θ decreases from 180 to 90 degrees. At θ = 90 degrees, terfuran and terthiophene exhibit the maximum HOMO-LUMO gap values of 5.54 and 5.01 eV, respectively. The maximum HOMO-LUMO gap arises from the absence of π orbital interactions between the adjacent five-membered rings due to orthogonality. Further decrease of θ from 90 degrees diminishes the gap. Despite the similar HOMO-LUMO gap trends observed for terfuran and terthiophene, the two oligomers exhibit substantial differences in their twisting potential energies (Figure 4(a)). As observed from Figure 4(a), the calculated barrier for the twisting of adjacent five-membered rings is 5.9 kcal/mol for terthiophene, while that for terfuran is 11.3

kcal/mol. The higher barrier for terfuran arises from the repulsion between the negative charges on oxygen atoms and π electrons on carbon atoms. These results indicate that terfuran assumes a planar structure with a rigid frameworks, whereas terthiophene shows five-membered rings that are slightly twisted away from the planar structure.[56] Similar results have been previously obtained by Gidoron et al.[8] The different twisting behaviors play a crucial role in determining the arrangement of π-conjugated oligomers inside a nanotube, as discussed below.

Single Terfuran Oligomer inside a Carbon Nanotube

We first determined local minima of the potential energy surface of a single terfuran inside an (*m*,*m*) nanotube (*m* is 8 or 10), as displayed in Figure 5. Independent of tube diameter, the optimized 1×3F@(*m*,*m*) structures in Figure 5 show a single inner terfuran located near the tube wall of a nanotube. Here, we estimated the interactions between the terfuran guest and a tube host by using the following equation,

$$E_{BE} = E_{total}(n\times 3F@(m,m)) - E_{total}((m,m)) - n \times E_{total}(3F) \quad (1)$$

where $E_{total}(n\times 3F@(m,m))$ is the total energy of an optimized $n\times 3F@(m,m)$ structure, $E_{total}((m,m))$ is that of the optimized (*m*,*m*) structure, $E_{total}(3F)$ is that of the optimized structure for single terfuran, and *n* is the number of terfurans contained in the (*m*,*m*) tube. Basis set superposition errors (BSSE)[57] were corrected for E_{BE} values listed in Table 1. Table 1 also presents E_{BE} values for corresponding $n\times 3T@(m,m)$ structures obtained in

a previous study.[32] Inspection of Table 1 shows that E_{BE} values for the two 1×3F@(*m*,*m*) structures are negative, indicating that host-guest interactions stabilize the 1×3F@(*m*,*m*) structures relative to the dissociation limit toward single terfuran and the (*m*,*m*) tube. The 1×3F@(*m*,*m*) structures have slightly smaller E_{BE} values than the corresponding 1×3T@(*m*,*m*) structures. These results indicate that the interactions between inner single terfuran and an (*m*,*m*) tube are weaker than those for the inner terthiophene case. As shown in Figures S1-1 and S1-2 (Supplementary information), there is a substantial number of contacts between H (C) atoms of the terfuran and C atoms of the tube at approximately 2.8 (3.5) Å, whose separations are optimal to operate attractive CH–π (π–π) interactions. Thus, the interactions between a single terfuran and a nanotube are due to the CH–π and π–π interactions. Because the CH–π and π–π interactions are long ranged, they do not significantly influence the migration of a π-conjugated oligomer inside a nanotube along the tube axis. In fact, as shown in Figure 6(I), the energy profiles of migration of single terfuran guest along the tube axis exhibit low barriers with 2.4 and 3.5 kcal/mol obtained for 1×3T@(8,8) and 1×3T@(10,10), respectively. Similarly, negligible migration barriers were found for 1×3T@(8,8) and 1×3T@(10,10) in Figure 6(II). Thus, our DFT calculations found that the π-conjugated oligomers can move smoothly inside a nanotube.

Multimeric Terfuran Oligomers inside a Carbon Nanotube

In this section, we discuss the properties of multimeric terfurans inside a nanotube. Optimized *n*×3F@(*m*,*m*) structures are given in Figure 7, together with the

E_{BE} values calculated according to Eq. (1). As shown in Figure 7, we found a variety of arrangements of multimeric terfurans inside a nanotube, depending on the number of chains and tube diameter. The negative E_{BE} values indicate that the host-guest materials in Figure 7 are energetically stable relative to the dissociation limit toward some terfurans and the nanotube. Reflecting a variety of inner terfuran arrangements, the E_{BE} values show a significant variation. By using the E_{BE} values in n×3F@(m,m) (Table 1), we can estimate the interchain interactions between the contained terfurans, as defined by the following equation.

$$E_{interact} = E_{BE}(n\times 3F@(m,m)) - n \times E_{BE}(1\times 3F@(m,m)) \quad (2)$$

Table 2 and Figure 7 list $E_{interact}$ values in the host-guest materials. The data presented in Table 2 and Figure 7 show that depending on n and m, the $E_{interact}$ values can be different signs. The negative (positive) $E_{interact}$ values indicate that the terfuran chains inside a nanotube interact attractively (repulsively). Table 2 shows that the absolute $E_{interact}$ values in n×3F@(8,8) are larger than those in n×3F@(10,10), suggesting that interchain interactions between terfurans are stronger within a smaller diameter tube. Thus, DFT calculations emphasize that tube-diameters strongly influence the magnitude of interchain interactions. Note that the magnitude of interchain interactions is important to determine migration behaviors of an inner terfuran within the 2×3F@(m,m) structures in terms of the energetics, as can be seen in Figure S2 (Supplementary Information).

Comparison of the data in Tables 1 and 2 found that $E_{interact}$ values at a certain structure are less significant than the host-guest interactions in 1×3F@(*m*,*m*) (E_{BE} value for 1×3F@(*m*,*m*)). Accordingly, the stronger host-guest (weaker guest-guest) interactions are a major (minor) factor for determining the arrangement of multimeric terfurans inside a nanotube. Because the inner space of the (10,10) tube is sufficiently large to accommodate two terfurans, both terfurans are located near the tube wall. The two terfurans are thus separated, and their interchain interactions are negligible. Substantial interchain interactions appear when the number of contained oligomers increases. Three terfurans encapsulated into the (10,10) tube interact with the tube wall as well as with the other terfurans. The $E_{interact}$ value for 3×3F@(10,10) is negative (Table 2), indicating that the interchain interactions are attractive. In contrast, a positive $E_{interact}$ value was obtained for 4×3F@(10,10). The different signs for the *n*×3F@(10,10) structures suggest that there is the optimal number of π-conjugated oligomers that can interact attractively with each other within a carbon nanotube (i.e., the optimal number of terfurans within the (10,10) tube is 3). Within the (8,8) tube with a smaller inner space, the optimal number is smaller. According to Table 2, the sign of $E_{interact}$ changes between 2×3F@(8,8) and 3×3F@(8,8). These results are helpful for understanding a recent experimental report finding that radial breathing vibrational frequencies of a nanotube containing multimeric π-conjugated oligomers exhibit a complex dependence on the nanotube diameter.[28]

Comparison between *n*×3F@(*m*,*m*) and *n*×3T@(*m*,*m*) in Interchain Interactions

Figure 7 shows that terfuran arrangements inside an (*m*,*m*) nanotube (*n*×3F@(*m*,*m*)) are similar to those of inner terthiophenes described in Ref. 32. Here, we compare the magnitudes of interchain interactions for *n*×3F@(*m*,*m*) and *n*×3T@(*m*,*m*). As observed in Table 2, the absolute $E_{interact}$ values for *n*×3F@(*m*,*m*) are smaller than the corresponding *n*×3T@(*m*,*m*) values, with the exception of quartarmer π-conjugated oligomers inside the (10,10) tube. An especially striking difference was found between 3×3F@(8,8) and 3×3T@(8,8): the absolute $E_{interact}$ value in the 3F case is 86.5 kcal/mol smaller than that in the 3T case. These results suggest that interchain interactions between terfuran oligomers inside tubes are weaker than those for the inner terthiophenes.

To understand the differences in the interchain interaction magnitudes of *n*×3F@(8,8) and *n*×3T@(8,8), we examine the π-conjugated oligomers' arrangements inside the (8,8) tube more closely. Figure 8 shows that the arrangements of π conjugated oligomers inside a nanotube depend on the type of contained heteroatoms. The dimer arrangements 2×3F@(8,8) and 2×3T@(8,8) are commonly cofacial, as depicted in Chart 2. However, these dimer structures have one oligomer shifting longitudinally by different distances from the original cofacial arrangement (longitudinal shift). In fact, the dimer arrangements in 2×3F@(8,8) and 2×3T@(8,8) can be distinguished by the longitudinal displacement from the original position (*y*(C)), as defined in Chart 2. The 2×3T@(8,8) structure shows a *y*(C) value of ~1.4 Å. In the slightly sliding arrangement, the HOMO-splitting of the terthiophene dimer is minimized, and thus the repulsion arising from the interchain orbital interactions is

diminished, as discussed in Ref. 32. In contrast, we found a significant longitudinal displacement in the terfuran dimer inside the (8,8) tube; one terfuran slides with respect to the other oligomer by 3.6 Å. Similarly, differences in the trimer arrangements can be observed for 3×3T@(8,8) and 3×3F@(8,8), with a slightly sliding arrangement for the terthiophenes and a significantly sliding arrangement for the terfuran case.

We now discuss the importance of the relative orientations of the multimeric terfurans for their energetics. For simplicity, we focused on the roles of dimer orientations in interchain interactions, as depicted in Chart 2. Figure S3 displays the total energy of longitudinally shifted cofacial 3F dimers as a function of the interchain spacing (z_{is}). Total energies relative to the dissociation limit toward two 3F oligomers ($E_{relative}$) were plotted. One local minimum with respect to z_{is} is present for each orientation of longitudinally shifted 3F dimers with a certain value (y(C))(see graphs in Figure S3). Each local minimum is described by two key parameters: the stabilization energy (E_{min}) and the optimal interchain spacing (z_{is}). We find that the E_{min} values are strongly dependent on the y(C) values, as shown in Figure 9(I). The most significant E_{min} value ($E_{min\text{-}opt}$: –9.8 kcal/mol) was found at y(C) = ~3.5 Å (Table 3). In the most stable shifted 3F dimer, the interchain spacing ($z_{is\text{-}opt}$) is 3.6 Å. Similar y(C)-dependent E_{min} values can be found in longitudinally-shifted 3T dimers (Figure 9(II)), as discussed in a previous report.[32] However, in the most stable shifted 3T dimer ($E_{min\text{-}opt}$ value of –9.3 kcal/mol), the terthiophene slides by only 1.5 Å from the original position. These scan analyses nicely explain the differences between terfuran and terthiophene dimers' orientation within a nanotube, as shown in Figure 8.

More interestingly, we found differences between the $E_{interact}$ and $E_{min\text{-}opt}$ values for 2×3F@(8,8), indicating that the nanotube encapsulation significantly perturbs the magnitude of the 3F interchain interactions. As mentioned above, the host-guest interactions are stronger than the guest-guest interactions. To maximize the host-guest interactions in 2×3F@(8,8), the terfuran guests are forced to deform.[58] The deformation of terfuran from its stable planar structure requires substantial energy according to Figure 3. The loss of planarity of inner terfurans[58] weakens the interchain interactions. In contrast, inner terthiophenes change from their local minimum to enhance their planarity without a substantial energy cost.[59] As a result, terthiophene can easily adjust its structure to maximize the host-guest interactions and the interchain interactions. Tables 2 and 3 actually show that the $E_{interact}$ value in 2×3T@(8,8) is the same as the corresponding $E_{min\text{-}opt}$ value, indicating that the tube encapsulation does not affect the magnitude of the 3T interchain interactions. These results clearly suggest that the deformation of π conjugated oligomers by the nanotube encapsulation plays an important role in determining the interchain interactions.

Factors in Determining the Arrangement of π-conjugated Oligomers inside a Tube

Finally, we summarize the key factors for determining the arrangement of π-conjugated oligomers inside a nanotube, as shown in Figure 10. The most dominant factor is the host-guest interaction arising from long-range CH–π and π–π interactions. Due to the long-range interactions, the inner single π-conjugated oligomer can move along the tube axis with a negligible barrier. Accordingly, the arrangement of

multimeric π-conjugated oligomers inside a nanotube is determined thermodynamically rather than kinetically. When a small number of π-conjugated oligomers are encapsulated into a large-diameter tube, host-guest interactions dominate the arrangement: the oligomers are located near the tube wall to maximize the host-guest interactions. On the other hand, multimeric π-conjugated oligomers inside a small-diameter tube are located near the tube wall, and they are near the other oligomers at the same time. In this situation, multimeric π-conjugated oligomers are oriented inside a nanotube to maximize the host-guest interactions as well as the guest-guest interactions (interchain interactions). Because stronger host-guest interactions are sufficient to deform the inner π-conjugated oligomers,[31] the magnitude of weaker interchain interactions is strongly affected by the nanotube encapsulation. The energy required by the deformation of the inner π-conjugated oligomers depends strongly on the oligomer type. The deformation of rigid terfurans by nanotube encapsulation leads to a high energy cost. The loss of inner terfuran planarity effectively diminishes their interchain interactions within the nanotube. In contrast, nanotube encapsulation enhances planarity of inner terthiophenes through host-guest interactions. Due to their flexible framework, the inner terthiophenes can easily adjust their structures to effectively optimize their interchain interactions. These results underline the dependence of interchain interaction magnitudes within a nanotube on the type of the encapsulated π-conjugated oligomers. Interchain interactions play an important role in determining the electronic properties of multimeric π-conjugated oligomers inside a nanotube, as detailed in Figure S4 (Supplementary information). Consequently, DFT calculations

revealed that depending on the type of the oligomer, nanotubes can modulate the electronic properties of inner π-conjugated oligomers.

Conclusions

Using density functional theory (DFT) including dispersion corrections (B97D functional), we investigated the arrangement of multimeric methyl-terminated terfurans inside a carbon nanotube. We then compared the results with those for the corresponding terthiophene cases to elucidate the factors determining the arrangement of π-conjugated oligomers inside a nanotube. DFT calculations found a variety of arrangements of multimeric terfuran chains inside a nanotube host, depending on the host diameter and the number of guests. The terfuran arrangement inside a larger-diameter tube is governed by attractive host-guest interactions due to CH–π and π–π interactions; these interactions induce the inner oligomers to be located near the tube wall. Within a smaller diameter tube, an inner terfuran sits near the tube wall and is located near the other terfurans at the same time. In this situation, the arrangement of multimeric terfurans is governed by the attraction arising from host-guest interactions as well as from the guest-guest (interchain) interactions. Because the interchain interactions are weaker than the host-guest interactions, the interchain interactions (host-guest interactions) are a minor (major) factor in the determination of the inner terfuran arrangement. Interestingly, the magnitude of interchain interactions is strongly affected by the deformation of π-conjugated oligomers by the stronger host-guest interactions. Nanotube encapsulation induces inner terfurans to lose their planarity,

weakening the interchain interactions. In contrast, terthiophenes contained inside a nanotube enhance their planarity, and thus their interchain interactions are maximized. As a result, differences in arrangements were found between multimeric terfurans and terthiophenes on the inside of a nanotube. Reflecting the different inner arrangements, π-conjugated oligomer chains interact differently. The interchain interactions that split the frontier orbitals of the multimeric π-conjugated oligomers are responsible for changing their electronic properties. Consequently, DFT calculations found that depending on types of oligomer, nanotube encapsulation has a strong impact on modulating the electronic properties of inner π-conjugated oligomers. Our DFT findings provide an effective guidance for devising a strategy for controlling the arrangement of π-conjugated oligomers in order to modulate their electronic properties.

Acknowledgements: The project was partially supported by a Grant-in-Aid for Young Scientists (B) from the Japan Society for the Promotion of Science (JSPS) (T. Y. at the Kyoto Institute of Technology, no. 26790001), and by a Grant-in-Aid for Scientific Research on the Innovative Area 'Stimuli-responsive Chemical Species for the Creation of Fundamental Molecules (No. 2408)' from the Ministry of Education, Culture, Sports, Science and Technology, Government of Japan (MEXT) (T.Y. at the Kyoto Institute of Technology, no. 15H00941).

Electronic supplementary information (ESI) available: origin of interactions between the single terfuran and a nanotube host (S1), migration of an inner terfuran

oligomer in 2×3T@(*m*,*m*) (S2), roles of the relative orientations of the cofacial terthiophene dimer in its energetics and optimal interchain spacings (S3), frontier orbitals based on multimeric terfurans in *n*×3F@(*m*,*m*) (S4), and full lists in Ref. 53. (S5). See DOI:

References and Notes

1 J. L. Brédas and G. B. Street, *Acc. Chem. Res.*, 1985, **18**, 309–315.

2 T. M. Swager, *Acc. Chem. Res.,* 1998, **31**, 201–207.

3 D. T. McQuade, A. E. Pullen and T. M. Swager, *Chem. Rev.*, 2000, **100**, 2537–2574.

4 M. Kertesz, C. H. Choi and S. Yang, *Chem. Rev.,* 2005, **105**, 3448–3481.

5 Z. Chen, C. S. Wannere, C. Corminboeuf, R. Puchta and P. v. R. Schleyer, *Chem. Rev.,* 2005, **105**, 3842–3888.

6 A. R. Murphy and J. M. J. Frechet, *Chem. Rev.,* 2007, **107**, 1066–1096.

7 C. Wang, H. Dong, W. Hu, Y. Liu and D. Zhu, *Chem. Rev*., 2012, **112**, 2208–2267.

8 O. Gidron, Y. Diskin-Posner and M. Bendikov, *J. Am. Chem. Soc.*, 2010, **132**, 2148–2150.

9 O. Gidron, N. Varsano, L. J. W. Shimon, G. Leitus and M. Bendikov, *Chem. Commun.,* 2013, **49**, 6256–6258.

10 O. Gidron and M. Bendikov, *Angew. Chem. Int. Ed.*, 2014, **53**, 2546–2555.

11 J. Cornil, D. Belionne, J.-P. Calbret and J. L. Brédas, *Adv. Mater.*, 2001, **13**, 1053–1067.

12 J. L. Brédas, J. P. Calbert, D. A. da Silva Filho and J. A. Cornil, *Proc. Natl. Acad. Sci. U.S.A.*, 2002, **99**, 5804–5809.

13 G. R. Hutchison, M. A. Ratner and T. J. Marks, *J. Am. Chem. Soc.*, 2005, **127**, 2339–2350.

14 G. R. Hutchison, M. A. Ratner and T. J. Marks, *J. Am. Chem. Soc.*, 2005, **127**, 16866–16881.

15 G. R. Hutchison, M. A. Ratner and T. J. Marks, *J. Phys. Chem.* B, 2005, **109**, 3126–3138.

16 S. E. Koh, C. Risko, D. A. da Silva Filho, O. Kwon, A. Facchetti, J. L. Brédas, T. J. Marks and M. A. Ratner, *Adv. Funct. Mater.,* 2008, **18**, 332–340.

17 A. N. Khobystov, D. A. Britz and G. A. D. Briggs, *Acc. Chem. Res.,* 2005, **38**, 901–909.

18 T. Takenobu, T. Takano, M. Shiraishi, Y. Murakami, M. Ata, H. Kataura, Y. Achiba and Y. Iwasa, *Nat. Mater.*, 2003, **2**, 683–688.

19 L.-J. Li, A. N. Khlobystov, J. G. Wiltshire, G. A. D. Briggs and R. J. Nicholas, *Nat. Mater.*, 2005, **4**, 481–485.

20 Y. Fujita, S. Bandow and S. Iijima, *Chem. Phys. Lett.*, 2005, **413**, 410–414.

21 Y. Yanagi, Y. Miyata and H. Kataura, *Adv. Mater.*, 2006, **18**, 437–441.

22 D. Nishide, H. Dohi, T. Wakabayashi, E. Nishibori, S. Aoyagi, M. Ishida, S. Kikuchi, R. Kitaura, T. Sugai, M. Sakata and H. Shinohara, *Chem. Phys. Lett.*, 2006, **428**, 356–360.

23 D. Nishide, T. Wakabayashi, T. Sugai, R. Kitaura, H. Kataura, Y. Achiba and H. Shinohara, *J. Phys. Chem.* C, 2007, **111**, 5178–5183.

24 M. A. Loi, J. Gao, F. Cordella, P. Blondeau, E. Menna, B. Bártová, C. Hébert, S. Lazar, G. A. Botton, M. Milko and C. Ambrosch-Draxl, *Adv. Mater.*, 2010, **22**, 1635–1639.

25 J. Gao, P. Blondeau, P. Salice, E. Menna, B. Bártová, C. Hébert, J. Leschner, U. Kaiser, M. Milko C. Ambrosch-Draxl and M. A. Loi, *Small*, 2011, **7**, 1807–1815.

26 L. Alvarez, Y. Almadori, R. Arenal, R. Babaa, T. Michel, R. Le. Parc, J.-L. Bantignies, B. Jousselme, S. Palacin, P. Hermet and J.-L. Sauvajol, *J. Phys. Chem.* C, 2011, **115**, 11898–11905.

27 M. Kalbáč, L. Kavan, S. Gorantla, T. Gemming and L. Dunsch, *Chem. Eur. J.*, 2010, **16**, 11753–11759.

28 Y. Almadori, L. Alvarez, R. Le. Parc, R. Aznar, F. Fossard, A. Loiseau, B. Jousselme, S. Campidelli, P. Hermet, A. Belhboub, A. Rahmani, T. Saito and J.-L. Bantignies, *J. Phys. Chem.* C, 2014, **118**, 19462–19468.

29 E. Gaufrés, N. Y.-Wa. Tang, F. Lapointe, J. Cabana, M.-A. Nadon, N. Cottenye, F. Raymond, T. Szkopek and R. Martel, *Nature Photonics*, 2014, **8**, 72–78.

30 S. Cambré, J. Campo, C. Beirnaert, C. Verlackt, P. Cool and W. Wenseleers, *Nature Nanotech.*, 2015, **10**, 248–252.

31 H. Yamashita and T. Yumura, *J. Phys. Chem.* C, 2012, **116**, 9681–9690.

32 T. Yumura and H. Yamashita, *J. Phys. Chem.* C, 2014, **118**, 5510–5522.

33 T. Yumura, K. Hirahara, S. Bandow, K. Yoshizawa and S. Iijima, *Chem. Phys. Lett.,* 2004, **386**, 38–43.

34 T. Yumura, S. Bandow, K. Yoshizawa and S. Iijima, *J. Phys. Chem.* B, 2004, **108**, 11426–11434.

35 T. Yumura, D. Nozaki, S. Bandow, K. Yoshizawa and S. Iijima, *J. Am. Chem. Soc.*, 2005, **127**, 11769–11776.

36 T. Yumura, M. Kertesz and S. Iijima, *J. Phys. Chem.* B, 2007, **111**, 1099–1109.

37 T. Yumura, M. Kertesz and S. Iijima, *Chem. Phys. Lett.,* 2007, **444**, 155–160.

38 T. Yumura and M. Kertesz, *J. Phys. Chem.* C, 2009, **113**, 14184–14194.

39 T. Yumura, *Phys. Chem. Chem. Phys.*, 2011, **13**, 337–346.

40 S. Grimme, *J. Comput. Chem.*, 2006, **27**, 1787-1799.

41 S. Grimme, *J. Chem. Phys.*, 2006, **124**, 034108.

42 A. D. Becke, *Phys. Rev.* A, 1988, **38**, 3098–3100.

43 A. D. Becke, *J. Chem. Phys*., 1993, **98**, 5648–5652.

44 P. J. Stephens, F. J. Devlin, C. F. Chabalowski and M. J. Frisch, *J. Phys. Chem.*, 1994, **98**, 11623–11627.

45 C. Lee, W. Yang and R. G. Parr, *Phys. Rev.* B, 1988, **37**, 785–789.

46 S. H. Vosko, L. Wilk and M. Nusair, *Can. J. Phys.,* 1980, **58**, 1200–1211.

47 T. C. Chung, J. H. Kaufman, A. J. Heeger and F. Wuld, *Phys. Rev.* B*,* 1984, **30**, 702–710.

48 M. Tachibana, S. Tanaka, Y. Yamashita and K. Yoshizawa, *J. Phys. Chem.* B, 2002, **106**, 3549–3556.

49 S. Yang, P. Olishevski and M. Kertesz, *Synth. Metals*, 2004, **141**, 171–177.

50 W. J. Hehre, R. Ditchfield and J. A. Popole, *J. Chem. Phys.*, 1972, **56**, 2257–2261.

51 R. Krishnan, J. S. Binkley, R. Seeger and J. A. Popole, *J. Chem. Phys*., 1980, **72**, 650–654.

52 T. Clark, J. Chandrasekhar, G. W. Spitznagel and P. v. R. Schleyer, *J. Comp. Chem*., 1983, **4**, 294–301.

53. M. J. Frisch, et al. Gaussian 09, Gaussian Inc.; Wallsingfold, CT, 2009.

54 J. P. Foster and F. Weinhold, *J. Am. Chem. Soc.*, 1980, **102**, 7211-7218.

55 D. F. Shriver and P. W. Atkins, *Inorganic Chemistry*, 4th ed.; Oxford University Press: Oxford, 2006.

56 The dihedral O–C–C–O angles in the optimized terfuran structure are ~180 degree. The dihedral S–C–C–S angles in the optimized terthiphene structure are ~166 degree.

57 S. F. Boys and F. Bernardi, *Mol. Phys*., 1970, **19**, 553-566.

58 The dihedral O–C–C–O angles of terfurans in 2×3F@(8,8) range from 170.6 to 172.5 degree. The value ranges, being similar those in 1×3F@(8,8) (~171.0 degree), are less than those in local minimum of methyl-terminated terfuran in the gas-phase (~180.0 degree). These changes indicate that host-guest interactions by nanotube encapsulation deforms inner terfurans, which costs ~1 kcal/mol per oligomer, to lose their planarity. Losing planarity of terfurans by the nantube encapsulation would diminish the magnitude of interchain interactions.

59 The dihedral S–C–C–S angles of terthiophenes in 2×3T@(8,8) have two values: 177.6 and 166.0 degree. The values of 166.0 degree, being close to those in local minimum of bare methyl-terminated terthiophene, were observed in five-membered rings of an oligomer close to methyl groups of the other oligomer. On the other hand, the values of 177.6 degree were observed in five-membered ring of an oligomer close to a five-membered ring of the other oligomer. These indicate that parts of five-membered rings gain planarity by nanotube encapsulation. See Ref. 31. Note that the guest deformation does not costs substantial energy (~0.3 kcal/mol per oligomer). In terms of the energy required by the guest deformation, the differences between terthiophene and terfurans can be understood from Figure 3. Gaining planarity of parts

of five-membered rings of terthiophene helps them to operate effectively interchain interactions.

Figure Captions

Fig. 1 Summary of the previous study discussing multimeric methyl-terminated terthiophenes inside a carbon nanotube.

Fig. 2 Schematic view of encapsulation of multimeric methyl-terminated terfurans into a carbon nanotube.

Fig. 3 Properties of (I) methyl-terminated terfuran and (II) methyl-terminated terthiophene. (a) B97-D optimized geometries in terms of bond length alternation, (b) frontier orbital features, and (c) atomic charges on contained heteroatoms, obtained from natural population analyses. The electronic properties in (b) and (c) were obtained from B3LYP single point calculations of the B97-D optimized π-conjugated oligomers.

Fig. 4 Twisting of adjacent five-membered rings around a connecting bond of (I) methyl-terminated terfuran and (II) methyl-terminated terthiophene in Fig. 3. (a) Twisting potential of a π-conjugated oligomer as a function of twisting angle θ (dihedral angle X–C–C–X, where X is O or S atom), based on B97-D calculations. (b) Changes of the HOMO-LUMO gap upon twisting of a π-conjugated oligomer. Orbital energies of frontier orbitals are obtained from B3LYP single point calculations of the twisting π-conjugated oligomers.

Fig. 5 B97-D optimized 1×3F@(*m*,*m*) structures where single terfuran is contained inside an (*m*,*m*) nanotube ((a) 1×3F@(8,8) and (b) 1×3F@(10,10)). The magnitude of interactions between single terfuran guest and a host nanotube is given by E_{BE} values in kcal/mol. Negative E_{BE} values indicate that the host-guest interactions are attractive.

Fig. 6 Energy profiles of migration of inner π-conjugated oligomer along the tube axis within the optimized 1×3F@(*m*,*m*) (I) or optimized 1×3T@(*m*,*m*) (II) structure in Fig. 5, obtained from B97-D calculations. The degree of migration of inner π-conjugated oligomer from its original position of an optimized structure is defined as *M*. Energies of π-conjugated oligomer migration in the inner spaces of the (8,8) and (10,10) tubes are given by circles and triangles, respectively.

Fig. 7 B97-D optimized *n*×3F@(*m*,*m*) structures where some terfurans are contained inside an (*m*,*m*) nanotube. Here *n* ranges from 2 to 4, and *m* is 8 or 10. The magnitude of interactions between multimeric terfuran guests and a host nanotube is also given as E_{BE} values in kcal/mol. Negative E_{BE} values indicate that host-guest interactions are attractive.

Fig. 8 Arrangement of inner π-conjugated oligomers in B97-D optimized *n*×3F@(8,8) and *n*×3T@(8,8) structures. (a) Dimer arrangements in the 2×3F@(8,8) and 2×3T@(8,8) structures, and (b) trimer arrangements in the 3×3F@(8,8) and 3×3T@(8,8) structures. Inner oligomers can be distinguished by different colors.

Fig. 9 Energetics of shifted terfuran (3F) dimers with orientation distinguished by the degree of longitudinal displacement of an oligomer from the original cofacial arrangement (y(C) as defined in Chart 2). Each shifted dimer orientation with a certain y(C) value has one local minimum that is stabilized relative to the dissociation limit to the two isolated oligomers. See Supplementary information for details (Figure S3). The stabilization energy in a local minimum is given by E_{min}. E_{min} values obtained from B97-D calculations are displayed as a function of y(C) in graph I. Similarly, y(C)-dependent E_{min} values in longitudinally shifted terthiophene (3F) dimers are given in graph II.

Fig. 10 Key factors in determination of the arrangement of multimeric π-conjugated oligomers inside a carbon nanotube.

Table 1. Estimation of host-guest interactions (E_{BE}) in B97D-optimized n×3F@(m, m) and n×3T@(m, m) structures,[a] where some methyl-terminated π-conjugated oligomers (terfuran (3F) or terthiophene (3T)) are on the inside of the (m, m) tube.

Host tube chirality	n [b]	3F guests [c]	3T guests [d]
(8,8)	1	–52.2	–57.8
(8,8)	2	–111.1	–125.1
(8,8)	3	–105.8	–36.1
(10,10)	1	–44.0	–48.5
(10,10) (I) [e]	2	–89.3	–101.5
(10,10) (II) [e]	2	–91.3	–102.5
(10,10)	3	–140.0	–156.7
(10,10)	4	–159.3	–191.2

[a] Optimized n×3F@(m, m) structures can be observed in Figure 7, and those in n×3F@(m, m) structures are taken from Ref. 32.
[b] n; the number of contained oligomers
[c] E_{BE} (in kcal/mol) in n×3F@(m, m): $E_{total}(n\times3F@(m,m)) - E_{total}((m,m)) - n \times E_{total}(3F)$
[d] Corresponding E_{BE} values (in kcal/mol) in n×3T@(m, m) are taken from Ref. 32.
[e] Labels (I) and (II) in 2×3T@(10, 10) can be observed in Figure 7.

Table 2. Estimation of guest-guest (interchain) interactions in B97D-optimized n×3F@(m, m) and n×3T@(m, m) structures,[a] where some methyl-terminated π-conjugated oligomers (terfuran (3F) or terthiophene (3T)) are on the inside of the (m, m) tube.

Host tube chirality	n [b]	3F guests [c]	3T guests [d]
(8,8)	2	–6.8	–9.6
(8,8)	3	50.7	137.2
(10,10) (I) [e]	2	–1.3	–4.5
(10,10) (II) [e]	2	–3.3	–5.5
(10,10)	3	–8.0	–11.1
(10,10)	4	16.7	2.8

[a] Optimized n×3F@(m, m) structures can be observed in Figure 7, and those in n×3F@(m, m) structures are taken from Ref. 32.
[b] n; the number of contained oligomers
[c] $E_{interact}$ (in kcal/mol) in n×3F@(m, m): $E_{BE}(n\times3F@(m,m) - n \times E_{BE}(1\times3F@(m,m))$
[d] Corresponding $E_{interact}$ values (in kcal/mol) in n×3T@(m, m) are taken from Ref. 32.
[e] Labels (I) and (II) in 2×3T@(10, 10) can be observed in Figure 7.

Table 3. Key parameters in the most stable structure of longitudinally-shifted cofacial dimers, consisted of terfurans (3F) or terthiophenes (3T).[a]

Key parameters	3F dimer [a]	3T dimer [a]
$E_{min\text{-}opt}$ [b]	–9.8	–9.3
$y_{min\text{-}opt}$ [c]	3.6	1.4
$z_{min\text{-}opt}$ [d]	3.3	3.6

[a] See detail discussion based on B97D calculations can be observed in Figure 9.
[b] $E_{min\text{-}opt}$ (in kcal/mol): the stabilization energy in the most stable structure of a longitudinally-shifted cofacial dimer, compared with the dissociation limit toward the two oligomers.
[c] $y_{min\text{-}opt}$ (Å): the longitudinal displacement of one oligomer from the original cofacial arrangement in the most stable orientation.
[d] $z_{min\text{-}opt}$ (Å): interchain spacing between terfurans in the most stable dimer orientation.

Table of contents entry

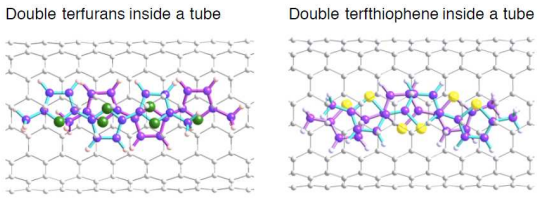

Dispersion corrected DFT calculations found different arrangements of π conjugated oligomers inside a carbon nanotube dependent on types of oligomer, which are responsible for determining their electronic properties.

Chart 1

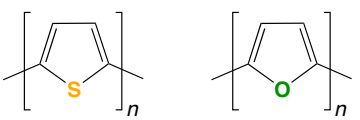

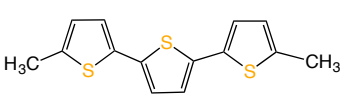

Methyl-terminated terthiophene

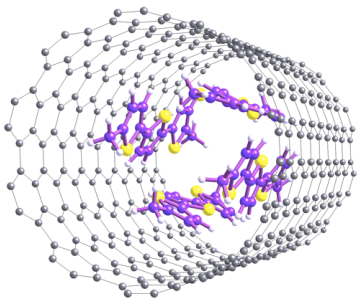

Methyl-terminated terthiophene inside a carbon nanotube

Fig. 1 Summary of the previous study discussing multimeric methyl-terminated terthiophenes inside a carbon nanotube.

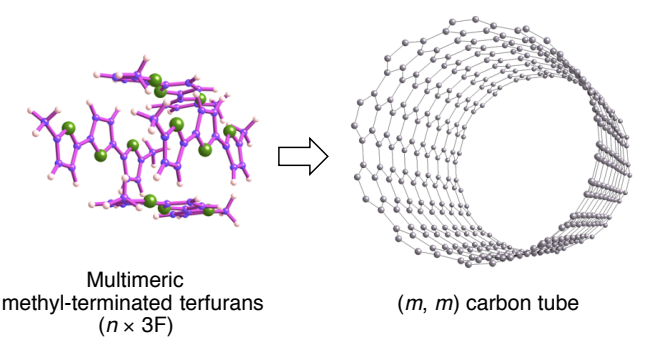

Fig. 2 Schematic view of encapsulation of multimeric methyl-terminated terfurans into a carbon nanotube.

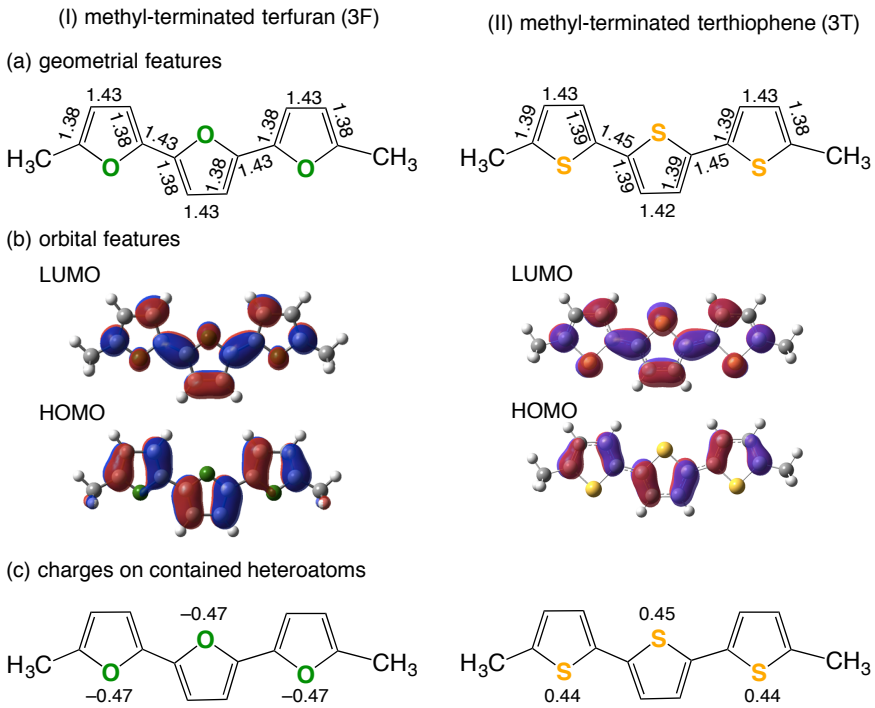

Fig. 3 Properties of (I) methyl-terminated terfuran and (II) methyl-terminated terthiophene. (a) B97-D optimized geometries in terms of bond length alternation, (b) frontier orbital features, and (c) atomic charges on contained heteroatoms, obtained from natural population analyses. The electronic properties in (b) and (c) were obtained from B3LYP single point calculations of the B97-D optimized π conjugated oligomers.

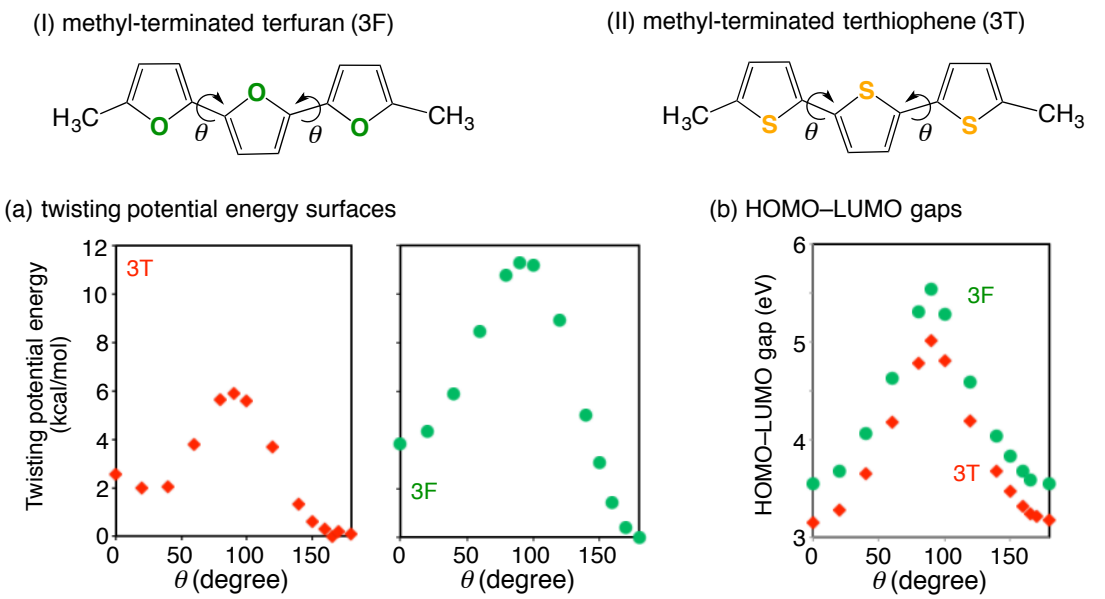

Fig. 4 Twisting of adjacent five-membered rings around a connecting bond of (I) methyl-terminated terfuran and (II) methyl-terminated terthiophene in Fig. 3. (a) Twisting potential of a π conjugated oligomer as a function of twisting angle θ (dihedral angle X–C–C–X, where X is O or S atom), based on B97-D calculations. (b) Changes of the HOMO–LUMO gap upon twisting of a π conjugated oligomer. Orbital energies of frontier orbitals are obtained from B3LYP single point calculations of the twisting π conjugated oligomers.

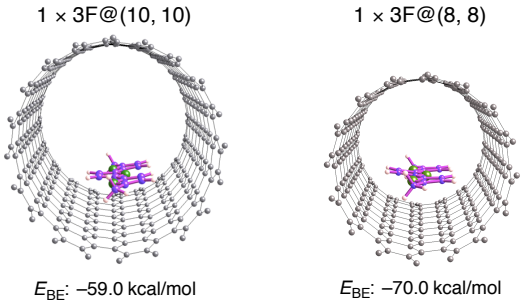

Fig. 5 B97D-optitmized 1 × 3F@(*m*,*m*) structures where single terfuran is contained inside a (*m*,*m*) nanotube ((a) 1 × 3F@(8,8) and (b) 1 × 3F@(10,10)). The magnitude of interactions between single terfuran guest and a host nanotube is given by E_{BE} values in kcal/mol. Negative E_{BE} values indicate that the host-guest interactions are attractive.

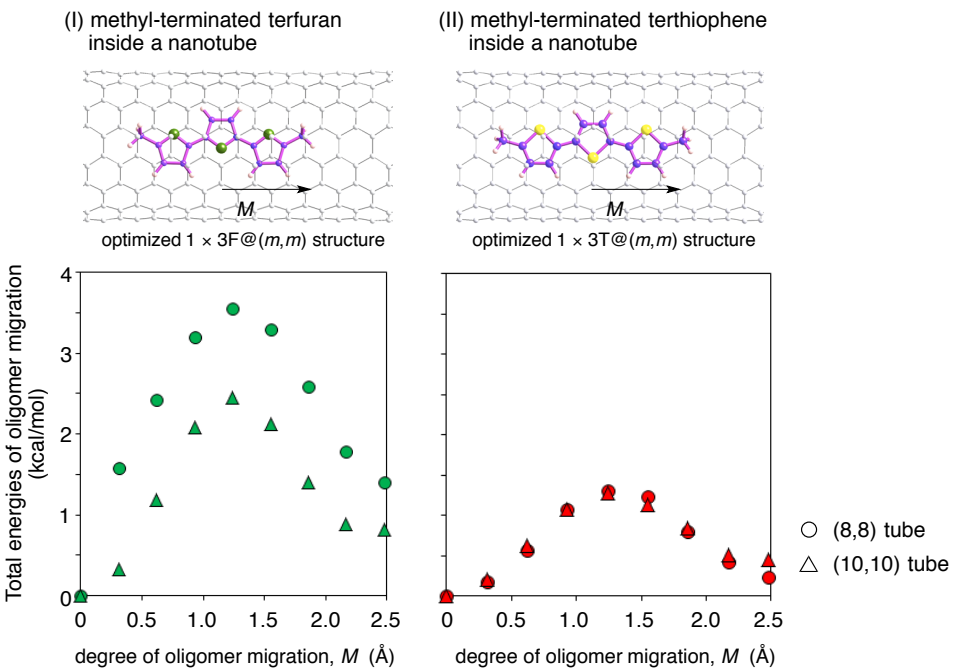

Fig. 6 Energy profiles of migration of inner π-conjugated oligomer along the tube axis within the optimized 1 × 3F@(*m*,*m*) structure (I) or optimized 1 × 3T@(*m*,*m*) (II) structure in Fig. 5, obtained from B97-D calculations. The degree of migration on inner π-conjugated oligomer from its original position of an optimized structure is defined as *M*. Energies of π-conjugated oligomer migration in the inner spaces of the (8,8) and (10,10) tubes are give by cricles and triangles, respectively.

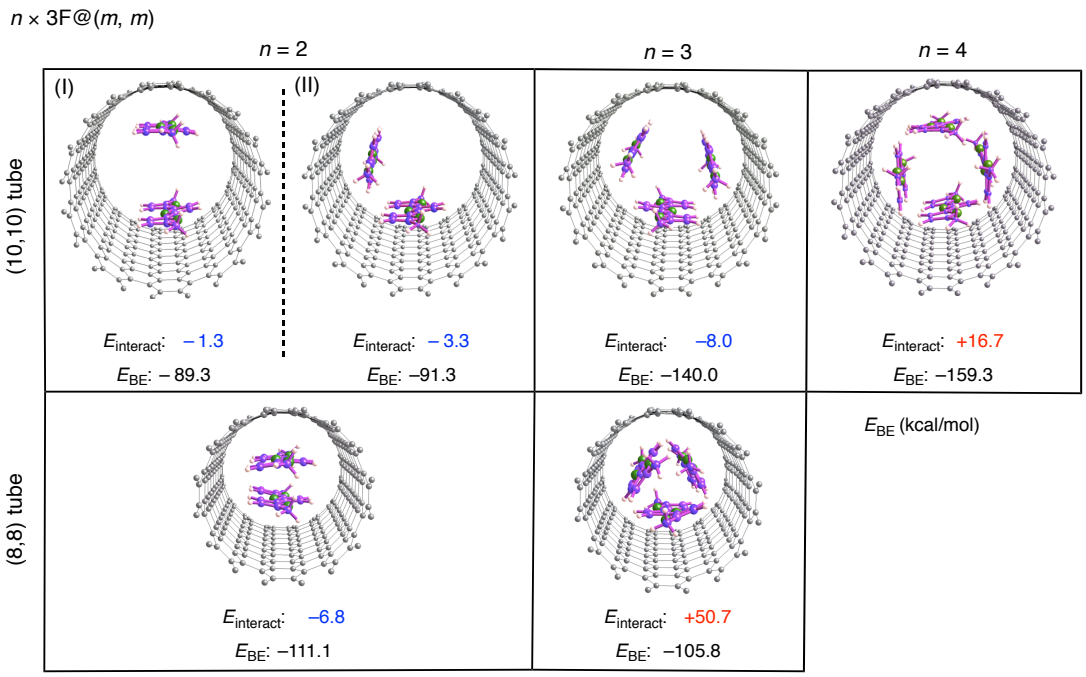

Fig. 7 B97D-optitmized $n \times 3F@(m,m)$ structures where some terfurans are contained inside an (m,m) nanotube. Here n ranges from 2 to 4, and m is 8 or 10. The magnitude of interactions between multimeric terfuran guests and a host nanotube is also given as E_{BE} values in kcal/mol. Negative E_{BE} values indicate that host-guest interactions are attractive.

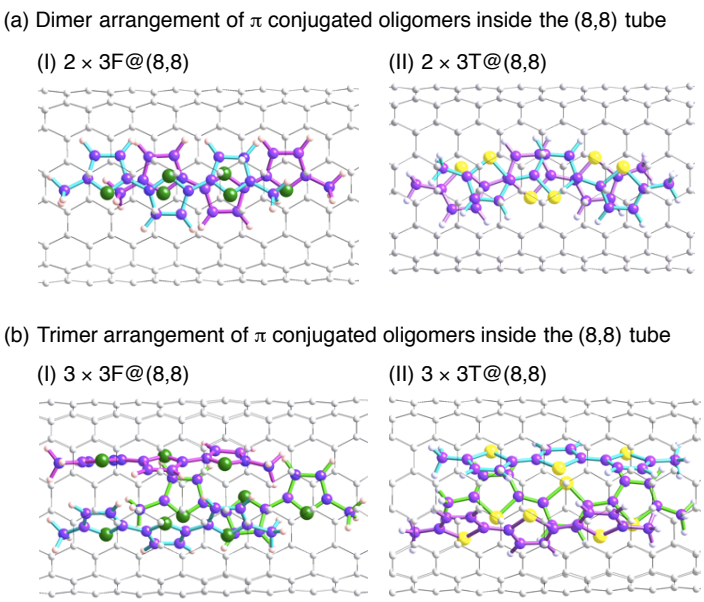

Fig. 8 Arrangement of inner π-conjugated oligomers in B97-D optimized $n \times$ 3F@(8,8) and $n \times$ 3T@(8,8) structures. (a) Dimer arrangements in the 2 × 3F@(8,8) and 2 × 3T@(8,8) structures, and (b) trimer arrangements in the 3 × 3F@(8,8) and 3 × 3T@(8,8) structures. Inner oligomers can be distinguished by different colors.

Chart 2

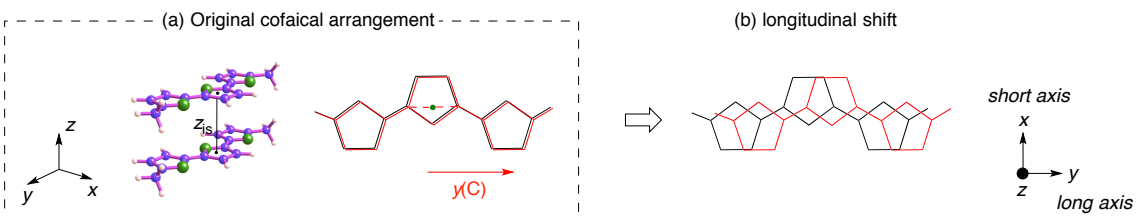

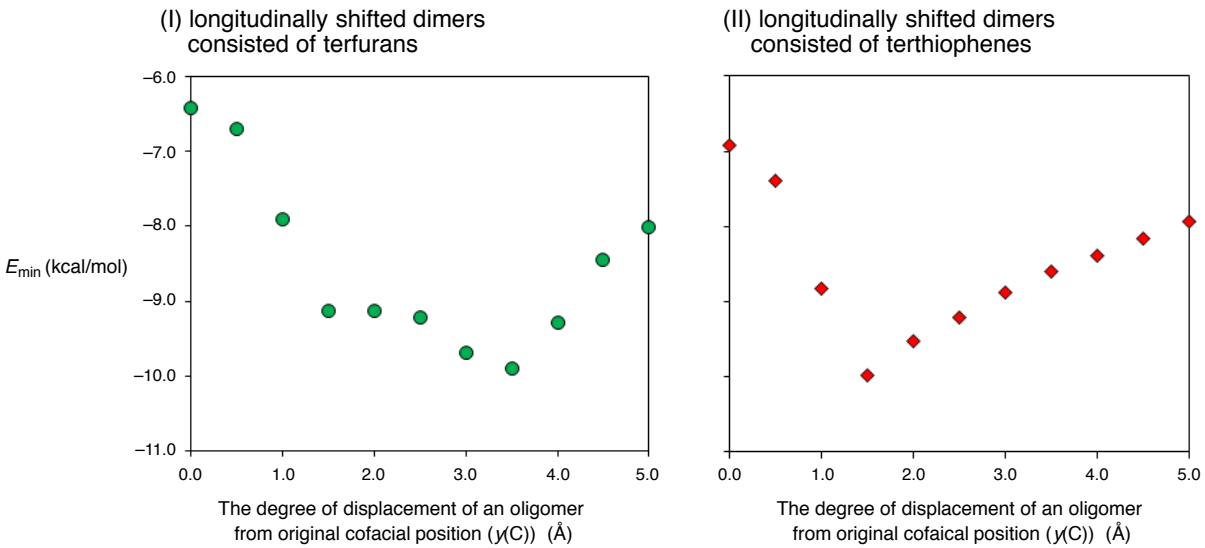

Fig. 9 Energetics of shifted terfuran (3F) dimers with orientation distinguished by the degree of longitudinal displacement of an oligomer from the origainal cofacial arrangement (y(C) as defined in Chart 2). Each shifted dimer oritentation with a certain y(C) value has one local minimum that is stabilized relative to the dissociation limit to the two isolated oligomers. See Supplementary information for details (Figure S3). The stabilization energy in a local minimum is given by E_{min}. E_{min} values obtained from B97-D calculations are displayed as a function of y(C) in graph I. Similarly, y(C)-dependent E_{min} values in longitudinally shifted terthiophene (3T) dimers are given in graph II.

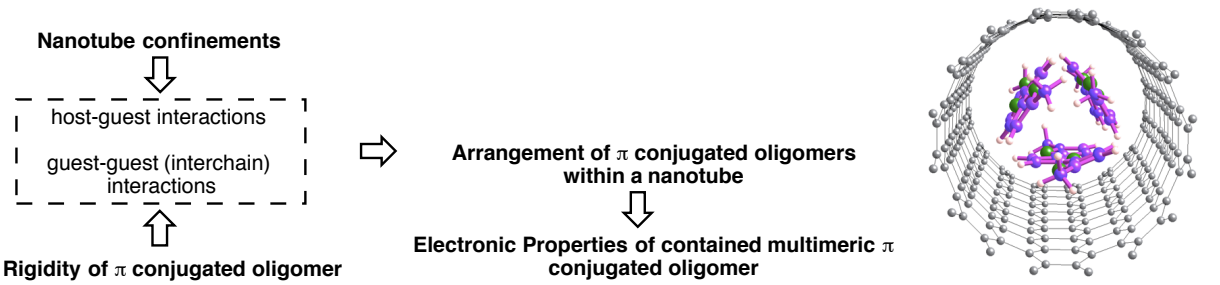

Fig. 10 Key factors in determination of the arrangement of multimeric π conjugated oligomers inside a carbon nanotube.